the morphological changes in neonatal female UGS have not yet been investigated.

Our results suggest that BPA has a stimulatory effect on in situ steroidogenesis in P1 UGS of both the male and female at low-dose exposure levels. Recently, ESRRG has been reported to bind strongly with BPA [35]. Susens et al. [36] have reported that expression of ESRRG in the mouse is organ-specific: ESRRG is expressed in the brain, heart, kidney, and skeletal muscle but not in the lung, spleen, and testis. In the present study, the up-regulation of *Cyp19a1* and *Cyp11a1* mRNA by BPA treatment was detected only in organs expressing *Esrrg* mRNA. These data suggest that the possibility of a stimulatory effect on in situ steroidogenesis by fetal exposure to low-dose BPA may be a concern not only in UGS but also in organs expressing ESRRG, such as the brain, heart, kidney, and ovary. It is important to note that Takeda et al. [23] have recently reported that ESRRG was detected in the human testis, suggesting that the distribution of ESRRG differs slightly between mice and humans.

In the present study, the BPA-specific up-regulation of steroidogenic enzyme mRNA in UGS, cerebellum, heart, kidney, and ovary was observed only during the neonatal period (i.e., P0 and P1) and not during the prenatal period (i.e., E17 and E18). During pregnancy in rodents, large amounts of estrogens produced in the maternal ovaries are continuously delivered to the fetus through the placenta. After birth, however, the fetus may be released from the maternal, high-estrogen environment. Thus, one possibility is that the maternal, high-estrogen environment in pregnancy may protect the fetus from the effect of BPA on in situ steroidogenesis during the prenatal period. However, we did not investigate the effects of neonatal BPA treatment on in situ steroidogenesis.

The EDC-induced alterations of the in situ estrogen environment depend on each compound. In addition to atrazine and dioxin, the organotin compound tributyltin also increases E_2 production in human placental choriocarcinoma cells [37]. Tributyltin has been demonstrated to induce the superimposition of male sex organs, such as a penis and/or a vas deferens, over female sex organs, which is a phenomenon known as imposex [38]. These studies suggest strongly that EDCs might affect fetal development not only by mimicking the actions of sex steroid hormones but also by alteration of in situ steroidogenesis.

In the prostate, AR expressed in mesenchyme is required for directing growth and branching morphogenesis of epithelia, presumably by induction of growth factors [39]. In the present study, fetal exposure to BPA or DES increased *Ar* mRNA expression in E17 UGM of the male, whereas *Esr1* mRNA expression was up-regulated in E17 UGM of the female. Recently, Richter et al. [40] have reported that in vitro BPA treatment stimulates *Ar* and *Esr1* mRNA expression in mesenchymal cells isolated from fetal mouse prostate. Thus, our results support the idea that BPA-induced cell proliferation of the primary prostatic ducts may be caused by inducing *Ar* mRNA expression in the male UGM. In contrast, the induction of *Esr1* mRNA expression by BPA or DES may create a positive-feedback loop in the female UGM. Further investigation and morphological analysis will be necessary to confirm the effects of up-regulated ESR1 in the female UGS.

In conclusion, we have shown the unique action of BPA in the mouse UGS. Specifically, we have demonstrated that the increases in E_2 levels and CYP19A1 (aromatase) activity were observed in the BPA-treated UGS but not in the DES-treated UGS. Ricke et al. [41] have recently reported that stromal hormone imbalance, a potential source of local E_2 production, may be responsible for prostatic disease, such as benign prostatic hyperplasia and prostate cancer. The data in the present study give rise to the concept that the development and differentiation of UGS in mouse fetuses is very sensitive to fetal exposure to low-dose BPA via the mother. Further investigation of various aspects of BPA-specific action is necessary to fully understand the role of BPA as an EDC.

ACKNOWLEDGMENTS

We thank Prof. Nobuhiro Harada at Department of Biochemistry, Fujita Health University School of Medicine, Aichi, Japan, for kindly providing rabbit polyclonal antiaromatase antibody. We also thank Mrs. Hiroko Nishii for technical support.

REFERENCES

1. Sekizawa J. Low-dose effects of bisphenol A: a serious threat to human health? J Toxicol Sci 2008; 33:389–403.
2. Newbold RR, Jefferson WN, Padilla-Banks E. Prenatal exposure to bisphenol A at environmentally relevant doses adversely affects the murine female reproductive tract later in life. Environ Health Perspect 2009; 117:879–885.
3. McPherson SJ, Ellem SJ, Risbridger GP. Estrogen-regulated development and differentiation of the prostate. Differentiation 2008; 76:660–670.
4. Welshons WV, Nagel SC, vom Saal FS. Large effects from small exposures. III. Endocrine mechanisms mediating effects of bisphenol A at levels of human exposure. Endocrinology 2006; 147:S56–S69.
5. Schonfelder G, Wittfoht W, Hopp H, Talsness CE, Paul M, Chahoud I. Parent bisphenol A accumulation in the human maternal-fetal-placental unit. Environ Health Perspect 2002; 110:A703–A707.
6. Tsutsumi O. Assessment of human contamination of estrogenic endocrine-disrupting chemicals and their risk for human reproduction. J Steroid Biochem Mol Biol 2005; 93:325–330.
7. Timms BG, Howdeshell KL, Barton L, Bradley S, Richter CA, vom Saal FS. Estrogenic chemicals in plastic and oral contraceptives disrupt development of the fetal mouse prostate and urethra. Proc Natl Acad Sci U S A 2005; 102:7014–7019.
8. Ogura Y, Ishii K, Kanda H, Kanai M, Arima K, Wang Y, Sugimura Y. Bisphenol A induces permanent squamous change in mouse prostatic epithelium. Differentiation 2007; 75:745–756.
9. Ho SM, Tang WY, Belmonte de Frausto J, Prins GS. Developmental exposure to estradiol and bisphenol A increases susceptibility to prostate carcinogenesis and epigenetically regulates phosphodiesterase type 4 variant 4. Cancer Res 2006; 66:5624–5632.
10. Markey CM, Luque EH, Munoz de Toro M, Sonnenschein C, Soto AM. In utero exposure to bisphenol A alters the development and tissue organization of the mouse mammary gland. Biol Reprod 2001; 65: 1215–1223.
11. Honma S, Suzuki A, Buchanan DL, Katsu Y, Watanabe H, Iguchi T. Low-dose effect of in utero exposure to bisphenol A and diethylstilbestrol on female mouse reproduction. Reprod Toxicol 2002; 16:117–122.
12. Kubo K, Arai O, Omura M, Watanabe R, Ogata R, Aou S. Low-dose effects of bisphenol A on sexual differentiation of the brain and behavior in rats. Neurosci Res 2003; 45:345–356.
13. Fan W, Yanase T, Morinaga H, Gondo S, Okabe T, Nomura M, Komatsu T, Morohashi K, Hayes TB, Takayanagi R, Nawata H. Atrazine-induced aromatase expression is SF-1 dependent: implications for endocrine disruption in wildlife and reproductive cancers in humans. Environ Health Perspect 2007; 115:720–727.
14. Baba T, Mimura J, Nakamura N, Harada N, Yamamoto M, Morohashi K, Fujii-Kuriyama Y. Intrinsic function of the aryl hydrocarbon (dioxin) receptor as a key factor in female reproduction. Mol Cell Biol 2005; 25: 10040–10051.
15. Moustafa GG, Ibrahim ZS, Hashimoto Y, Alkelch AM, Sakamoto KQ, Ishizuka M, Fujita S. Testicular toxicity of profenofos in matured male rats. Arch Toxicol 2007; 81:875–881.
16. Song KH, Lee K, Choi HS. Endocrine disrupter bisphenol A induces orphan nuclear receptor Nur77 gene expression and steroidogenesis in mouse testicular Leydig cells. Endocrinology 2002; 143:2208–2215.
17. Mlynarcikova A, Kolena J, Fickova M, Scsukova S. Alterations in steroid hormone production by porcine ovarian granulosa cells caused by bisphenol A and bisphenol A dimethacrylate. Mol Cell Endocrinol 2005; 244:57–62.
18. Hojo Y, Higo S, Ishii H, Ooishi Y, Mukai H, Murakami G, Kominami T, Kimoto T, Honma S, Poirier D, Kawato S. Comparison between

hippocampus-synthesized and circulation-derived sex steroids in the hippocampus. Endocrinology 2009; 150:5106–5112.
19. Nakanishi T, Nishikawa J, Hiromori Y, Yokoyama H, Koyanagi M, Takasuga S, Ishizaki J, Watanabe M, Isa S, Utoguchi N, Itoh N, Kohno Y, et al. Trialkyltin compounds bind retinoid X receptor to alter human placental endocrine functions. Mol Endocrinol 2005; 19:2502–2516.
20. Kanno J, Aisaki K, Igarashi K, Nakatsu N, Ono A, Kodama Y, Nagao T. "Per cell" normalization method for mRNA measurement by quantitative PCR and microarrays. BMC Genomics 2006; 7:64–77.
21. Ishii K, Imanaka-Yoshida K, Yoshida T, Sugimura Y. Role of stromal tenascin-C in mouse prostatic development and epithelial cell differentiation. Dev Biol 2008; 324:310–319.
22. Jakab RL, Horvath TL, Leranth C, Harada N, Naftolin F. Aromatase immunoreactivity in the rat brain: gonadectomy-sensitive hypothalamic neurons and an unresponsive "limbic ring" of the lateral septum-bed nucleus-amygdala complex. J Steroid Biochem Mol Biol 1993; 44:481–498.
23. Takeda Y, Liu X, Sumiyoshi M, Matsushima A, Shimohigashi M, Shimohigashi Y. Placenta expressing the greatest quantity of bisphenol A receptor ERRgamma among the human reproductive tissues: predominant expression of type-1 ERRgamma isoform. J Biochem 2009; 146:113–122.
24. vom Saal FS, Akingbemi BT, Belcher SM, Birnbaum LS, Crain DA, Eriksen M, Farabollini F, Guillette LJ Jr, Hauser R, Heindel JJ, Ho SM, Hunt PA, et al. Chapel Hill Bisphenol A Expert Panel Consensus Statement: integration of mechanisms, effects in animals and potential to impact human health at current levels of exposure. Reprod Toxicol 2007; 24:131–138.
25. Steinmetz R, Mitchner NA, Grant A, Allen DL, Bigsby RM, Ben-Jonathan N. The xenoestrogen bisphenol A induces growth, differentiation, and c-fos gene expression in the female reproductive tract. Endocrinology 1998; 139:2741–2747.
26. Milligan SR, Balasubramanian AV, Kalita JC. Relative potency of xenobiotic estrogens in an acute in vivo mammalian assay. Environ Health Perspect 1998; 106:23–26.
27. Colerangle JB, Roy D. Profound effects of the weak environmental estrogen-like chemical bisphenol A on the growth of the mammary gland of Noble rats. J Steroid Biochem Mol Biol 1997; 60:153–160.
28. Kawato S. Endocrine disrupters as disrupters of brain function: a neurosteroid viewpoint. Environ Sci 2004; 11:1–14.
29. Donjacour AA, Cunha GR. Stromal regulation of epithelial function. Cancer Treat Res 1991; 53:335–364.
30. Hayashi N, Cunha GR, Parker M. Permissive and instructive induction of adult rodent prostatic epithelium by heterotypic urogenital sinus mesenchyme. Epithelial Cell Biol 1993; 2:66–78.
31. Thomson AA. Role of androgens and fibroblast growth factors in prostatic development. Reproduction 2001; 121:187–195.
32. Timms BG, Lee CW, Aumuller G, Seitz J. Instructive induction of prostate growth and differentiation by a defined urogenital sinus mesenchyme. Microsc Res Tech 1995; 30:319–332.
33. Cunha GR. Age-dependent loss of sensitivity of female urogenital sinus to androgenic conditions as a function of the epithelia-stromal interaction in mice. Endocrinology 1975; 97:665–673.
34. Thomson AA, Timms BG, Barton L, Cunha GR, Grace OC. The role of smooth muscle in regulating prostatic induction. Development 2002; 129: 1905–1912.
35. Takayanagi S, Tokunaga T, Liu X, Okada H, Matsushima A, Shimohigashi Y. Endocrine disruptor bisphenol A strongly binds to human estrogen-related receptor gamma (ERRgamma) with high constitutive activity. Toxicol Lett 2006; 167:95–105.
36. Susens U, Hermans-Borgmeyer I, Borgmeyer U. Alternative splicing and expression of the mouse estrogen receptor-related receptor gamma. Biochem Biophys Res Commun 2000; 267:532–535.
37. Nakanishi T, Kohroki J, Suzuki S, Ishizaki J, Hiromori Y, Takasuga S, Itoh N, Watanabe Y, Utoguchi N, Tanaka K. Trialkyltin compounds enhance human CG secretion and aromatase activity in human placental choriocarcinoma cells. J Clin Endocrinol Metab 2002; 87:2830–2837.
38. Horiguchi T. Masculinization of female gastropod mollusks induced by organotin compounds, focusing on mechanism of actions of tributyltin and triphenyltin for development of imposex. Environ Sci 2006; 13:77–87.
39. Cunha GR, Donjacour A. Stromal-epithelial interactions in normal and abnormal prostatic development. Prog Clin Biol Res 1987; 239:251–272.
40. Richter CA, Taylor JA, Ruhlen RL, Welshons WV, Vom Saal FS. Estradiol and bisphenol A stimulate androgen receptor and estrogen receptor gene expression in fetal mouse prostate mesenchyme cells. Environ Health Perspect 2007; 115:902–908.
41. Ricke WA, McPherson SJ, Bianco JJ, Cunha GR, Wang Y, Risbridger GP. Prostatic hormonal carcinogenesis is mediated by in situ estrogen production and estrogen receptor alpha signaling. FASEB J 2008; 22: 1512–1520.

J Gastroenterol (2011) 46:339–349
DOI 10.1007/s00535-010-0355-9

ORIGINAL ARTICLE—ALIMENTARY TRACT

CITED2 is activated in ulcerative colitis and induces p53-dependent apoptosis in response to butyric acid

Tsutomu Yoshida · Tsukasa Sekine · Ken-ichi Aisaki · Tetuo Mikami · Jun Kanno · Isao Okayasu

Received: 13 June 2010 / Accepted: 21 November 2010 / Published online: 17 December 2010

Abstract
Background In ulcerative colitis (UC), *Fusobacterium varium* is significantly detected in patients' mucosa, and butyric acid (BA), abundantly produced by the bacterium, activates the p53 system and induces epithelial apoptosis, as we previously reported. However, factors active in the link between BA and p53 have yet to be clarified. Here, we identified a gene activated by BA specifically in UC-associated cancer cell lines and ascertained the mechanism of its activation of p53.
Methods cDNA microarray analysis based on the Percellome (per cell normalization) method was performed on BA-stimulated UC-associated cancers and sporadic colorectal cancer cell lines under conditions mimicking colonic epithelium UC. For validation of microarray results, molecular, biochemical, and histopathological analyses were performed.
Results We found the CBP/p300-interacting transactivator with glutamic acid/asparagine-rich carboxy-terminal domain 2 (CITED2) to be specifically upregulated in UC-associated cancer cell lines by BA treatment, at both mRNA and protein expression levels. CITED2 could be shown to induce p53 acetylation and p53-dependent apoptosis, accompanied by binding of CBP/p300. BA-dependent apoptosis was suppressed by an inhibitor of monocarboxylate transporter-1 and an siRNA for p53. In inflammatory foci of UC, histologically evident inflammatory activity and CITED2 expression were significantly correlated.
Conclusions CITED2 was identified as UC-associated protein by cDNA microarray based on the Percellome method under UC-mimicking conditions in vitro. CITED2 activation may induce mucosal apoptosis and erosion by activating p53 and thus play a critical role in linking enteric bacteria with mucosal inflammation in UC.

Keywords Ulcerative colitis · Inflammation · Apoptosis · CITED2 · Butyric acid · p53 · CBP/p300

The GeneChip data have been deposited in the Percellome project site (http://www.nihs.go.jp/tox/TtgPublication.htm) and are accessible with no restriction.

Electronic supplementary material The online version of this article (doi:10.1007/s00535-010-0355-9) contains supplementary material, which is available to authorized users.

T. Yoshida (✉) · T. Sekine · T. Mikami · I. Okayasu
Department of Pathology, Kitasato University School of Medicine, 1-15-1 Kitasato, Minami-ku, Sagamihara, Kanagawa 252-0374, Japan
e-mail: tyoshida@med.kitasato-u.ac.jp

K. Aisaki · J. Kanno
Division of Cellular and Molecular Toxicology, National Institute of Health Sciences, 1-18-1 Kamiyoga, Setagaya-ku, Tokyo 158-5801, Japan

Abbreviations

BA	Butyric acid
CITED2	CBP/p300-interacting transactivator with glutamic acid/asparagine-rich carboxy-terminal domain 2
4CHC	4-Hydroxycinnamate
IL-10	Interleukin-10
MCT1	Monocarboxylate transporter-1
q-RT-PCR	Quantitative reverse transcription PCR
sCRC	Sporadic colorectal cancer
UC	Ulcerative colitis
UCCA	Ulcerative colitis-associated cancer

Introduction

Ulcerative colitis (UC) is an intractable inflammatory bowel disease whose etiology is not known in detail. With long-standing UC, adenocarcinomas tend to occur in the colon, which might be due to repeated episodes of active chronic inflammation and remission [1, 2]. In a murine model system, dextran sulfate sodium (DSS) without mutagenicity induces UC-like colitis [3], and long-term repeated treatment with DSS can induce colitic cancers [4, 5]. Therefore, UC can be considered as a model disease for carcinogenesis on a background of chronic inflammation, and elucidation of the etiology of UC is important for treatment and prevention purposes.

The bacterial flora seem to constitute an important factor for triggering inflammation in UC, in accordance with previous reports concerning spontaneous development of UC-like colitis in IL-10 knockout mice under conventional breeding but not germ-free conditions [6–8]. Previously, we detected *Fusobacterium varium* (*F. varium*) by direct culture of mucosal biopsy specimens of UC patients and found intraepithelial invasion of *F. varium* to result in production of inflammatory cytokines in colonic epithelial cell lines in vitro [9, 10]. *F. varium* produces a short-chain fatty acid, butyric acid (BA), and direct luminal injection of BA into the rectum was found to induce apoptosis and UC-like lesions in mice [11]. In addition, BA activates p53-dependent apoptosis and DNA repair in vitro, and activation of p53 by its phosphorylation has been observed in situ in inflammatory foci of UC patients [12]. Clinically, we have shown significant improvement of UC by antibiotic combination therapy targeting *F. varium* [13, 14]. Recently, this was confirmed by a double-blind, placebo-controlled, multicenter trial [15]. However, the molecular mechanisms of BA-mediated p53 activation are unknown and largely remain to be elucidated.

In order to clarify this issue, we compared the genetic profiles of UC-associated carcinoma (UCCA) and sporadic colorectal adenocarcinoma (sCRC) cell lines undergoing BA treatment. Both series of cell lines were established in our laboratory [16]. The former include both p53 wild and mutant cells, whereas the latter are p53 wild. BA upregulates early response genes especially in UCCA cell lines, acting upstream of p53. Using whole genome cDNA microarray chips and the "per cell" normalization method (Percellome method) [17], we here identified genes specifically upregulated in UCCA lines with BA treatment. By detailed validation and the further examination, we focused on one upregulated gene, encoding the CBP/p300-interacting transactivator with glutamic acid/asparagine-rich carboxy-terminal domain 2 (CITED2) [18]. The protein itself activates p53 and its downstream molecules and accelerates apoptosis, and histological analysis revealed unique expression in the colonic mucosa of UC patients. Thus, we consider that CITED2 is an important and specific mediator of inflammation in UC, and might thus serve as a target of therapy.

Materials and methods

Cell lines and clinical cases

The human UCCA cell lines UCCA21, UCCA22, UCCA23, UCCA24, UCCA25 (p53 wild), and UCCA3 (p53 mutant), and the sCRC cell lines KE24, KE43w, and KE43p (p53 wild) were established in our laboratory [16], and cultured in Dulbecco's Modified Eagle Medium (GIBCO, Carlsbad, CA, USA) supplemented with 10% fetal bovine serum containing penicillin and streptomycin (GIBCO) at 37°C in 5% CO_2.

Microarray and data analysis

GeneChip analysis was conducted according to the Percellome method [17, 19] described in the Electronic Supplementary Material in detail. The GeneChip data have been deposited in the Percellome project site (http://www.nihs.go.jp/tox/TtgPublication.htm) and are accessible with no restriction. Differentially expressed genes were extracted by Fx algorithm [20], described in the Supplementary Methods online.

q-RT-PCR and western blotting

Total RNA was isolated from cells with an RNeasy kit (QIAGEN, Hilden, Germany), and 2-μg aliquots were used to synthesize cDNAs with a High Capacity cDNA Reverse Transcription Kit (Applied Biosystems, Foster City, CA, USA). Pre-amplified DNAs generated with a TaqMan PreAmp Master Mix Kit (Applied Biosystems) were used as templates for quantitative PCR with TaqMan Gene Expression Master Mix (Applied Biosystems) and FAM-dye-labelled TaqMan probe and primer sets for β-actin, CITED2, p53, CDKN1A (p21), Bax, MCT1, p53R2 (Applied Biosystems) using the 7500 real-time PCR system (Applied Biosystems). Quantitative PCR was performed as multiplex PCR with a VIC-dye-labelled β-actin probe and the fold ratio against VIC-labeled β-actin was calculated. All the quantitative RT-PCR (q-RT-PCR) studies were performed in triplex, and representative results for three independent experiments are shown.

Aliquots of 2×10^6 UCCA24 or KE43p cells after various treatments were lysed with lysis buffer (20 mM Tris–HCl, pH 7.6, 170 mM NaCl, 1 mM EDTA, 0.5% NP-40, 1 mM dithiothreitol). After separation by 12% SDS-

polyacrylamide gel electrophoresis and protein transfer to polyvinyl membranes, blocking with 5% bovine serum albumin was performed. Antibodies for CITED2 (Novous Biologicals, Inc Littleton, CO, USA), p53 (Novocastra Laboratories, Newcastle upon Tyne, UK), acetylated-p53 (Bio Academia, Osaka, Japan), $p21^{Cip1}$ (Santa Cruz Biotechnology, Santa Cruz, CA, USA), Bax (Transduction Laboratories, Lexington, KY, USA), and CBP/p300 (Santa Cruz) were used as first antibodies for western blotting. HRP-conjugated anti-mouse or HRP-conjugated anti-rabbit antibodies were then employed as secondary antibodies with ECL Western Blotting Detection Reagents (GE Healthcare, Buckinghamshire, UK) for visualization. Densitometry was performed by using ImageJ software (National Institutes of Health, USA)

Transfection and RNAi (siRNA) assays

Human CITED2 cDNA was obtained from Open Biosystems (Thermo Fisher Scientific, Huntsville, AL, USA, clone: LIFESEQ8724402) and subcloned into pcDNA-DEST40 (Invitrogen). Human CBP/p300 cDNA was also subcloned into the pcDNA-DEST40 vector. Transfection into UCCA24 and KE43p was achieved with Lipofectamin2000 (Invitrogen). siRNAs for CDKN1A, CITED2, HOXA1, SAT, TUBA3, and p53 (Ambion, Austin, TX, USA), and for non-sense control (Ambion) were transfected with the siPORT NeoFX Transfection Agent (Ambion).

Butyric acid treatment, detection of apoptosis, and MCT1 inhibition assays

Cultured cells were exposed to 2.5 mM BA as previously described [12]. Apoptosis was detected by the TUNEL method visualized by fluorescein isothiocyanate (FITC)-labeled digoxigenin according to the manufacturer's protocol with slight modifications using an ApopTag Plus Peroxidase In Situ Apoptosis Detection Kit (Intergen, Purchase, NY, USA). Apoptotic cells were counted and the percentages versus more than 100 DAPI (4′,6-diamino-2-phenylindole) positive cells were calculated. 0.5 mM 4-hydroxycinnamate (4CHC, Sigma, Saint Louis, MO, USA) was added to the culture medium for MCT1 inhibition assays.

Immunoprecipitation

Aliquots of 2×10^7 UCCA24 and KE43p cells were lysed in 1 ml of TNE buffer (10 mM Tris–HCl, pH 7.8, 1% nonidet-P 40, 0.15 M NaCl, 1 mM EDTA). After preprecipitation with protein G-Sepharose for 1 h at 4°C, lysates were incubated with 1 μg of anti-CITED2 antibody or anti-CBP/p300 for 1 h at 4°C followed by incubation with protein G-Sepharose for 1 h at 4°C. After centrifugation at 15,000 rpm for 5 min, the precipitants were washed with TNE buffer 5 times and denatured at 95°C. After SDS-polyacrylamide gel electrophoresis, they were subjected to western blotting with anti-CBP/p300 or anti-CITED2 antibodies.

Colorectal specimens and immunohistochemistry

A total of 102 surgically resected colorectal specimens from active and inactive UC patients and 20 from diverticulitis patients were obtained from the files of Kitasato University East Hospital and Kitasato University Hospital, and the histological activity of UC was determined according to the Matts' classification [21]: score 1, normal appearance; score 2, some infiltration of neutrophils in the mucosa; score 3, much cellular infiltration or presence of cryptitis; score 4, presence of crypt abscess and cellular infiltration; and score 5, presence of ulceration, erosion or necrosis, and cellular infiltration. Diverticulitis activity in diverticulosis was evaluated as none to mild and severe. Specimens were fixed with 10% formalin and embedded in paraffin. Semi-serial 4-μm-thick sections were cut for hematoxylin–eosin (H&E) staining and CITED2 immunohistochemistry with monoclonal anti-CITED2 antibodies (JA22, 1/1000, Novus Biologicals, Inc., Littleton, CO, USA) and an EnVision + kit (DakoCytomation, Glostrup, Denmark). After blocking endogenous peroxidase with 0.3% H_2O_2 in methanol, a 15-min microwave pretreatment in citrate buffer (pH 6.0, 0.01 mol/l) was performed for antigen retrieval, and after incubation with anti-CITED2 antibodies for 1 h at room temperature. 3,3′-Diaminobenzidine was applied as the final chromogen and faint nuclear counterstaining was finally achieved with methyl green. Scoring of immunoreactivity was performed as reported by Sinicrope et al. [22], and statistically analyzed by the Spearman's rank correlation test and Mann–Whitney's *U* test.

Results

Butyric acid upregulates the transcriptional expression of CITED2 specifically in UCCA lines

To identify genes upregulated by BA treatment specifically in UCCA lines, three UCCA and three sCRC lines were treated with 2.5 mM of BA (pH 7.4 in the culture medium). We earlier reported that the concentration of BA in the wells of Vero cell culture with *F. varium* was 6.42 mM (pH 6.90) [11], and 2.5 mM induced p53-mediated DNA repair [12]. The Percellome method enabled us to compare the mRNA expression profiles among the different cell lines per cell based on DNA content of each biosample. We applied the original algorithm (Fx) [20] and upregulated and

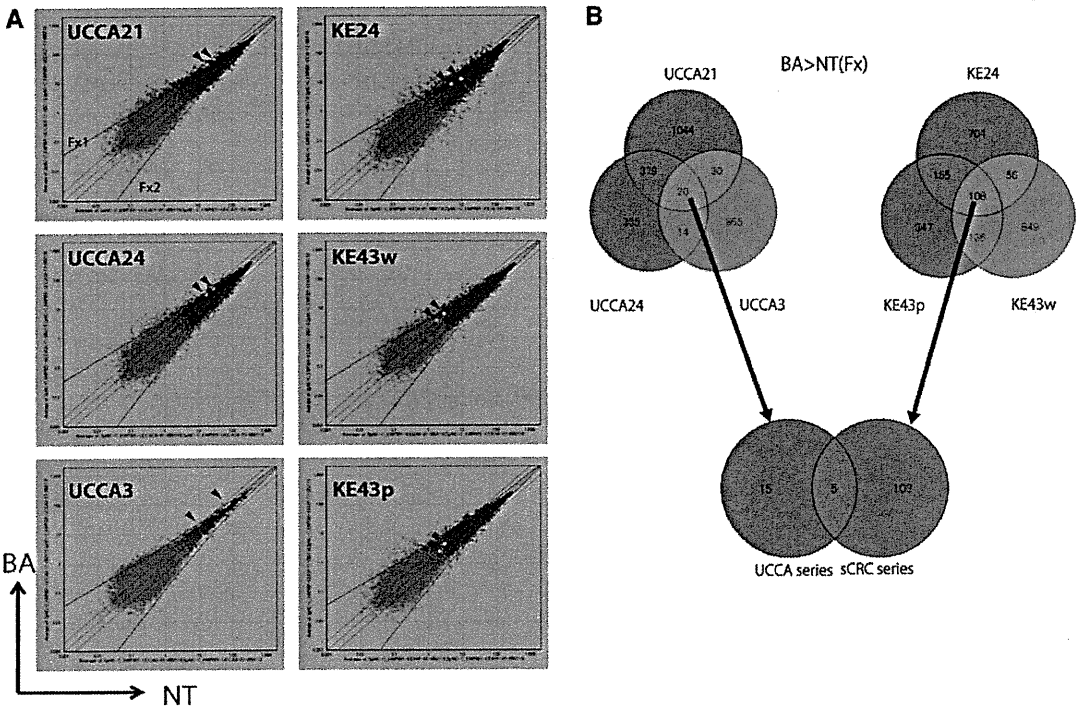

Fig. 1 **a** Genome-wide expression analysis after BA treatment. The analysis was performed by using the Affymetrix GeneChip Human Genome U133 plus 2.0 Array. Scatter plots are shown for BA treatment (BA) for 24 h and non-treatment (NT). The *open circles* show expression levels for each probe set. The *colors* indicate probabilities provided by the Affymetrix GeneChip Operation System: *red* means good and *green* means poor. The *yellow circles* show CITED2 probe sets for areas highlighted by *arrowheads*. The *black lines* show twofold, onefold, and 0.5-fold, respectively, and the *blue lines* indicate the empirical threshold levels (Fx1 and Fx2). The *spots above* the Fx1 and *below* the Fx2 line were evaluated as upregulated and downregulated, respectively ($p < 0.02$). **b** Venn diagrams of the upregulated probe sets in butyric acid (BA) treatment compared with non-treated (NT) controls in UCCA lines (UCCA21, UCCA24, and UCCA3) and sCRC lines (KE24, KE43p, and KE43w). *Numbers* of upregulated probe sets are indicated. Among the 20 and 108 probe sets upregulated in the UCCA and sCRC series, respectively, 5 were commonly upregulated in both. *Fx* Fx algorithm for the empirical threshold calculation

downregulated genes were listed at $p < 0.02$ (Fig. 1a). As compared with non-treated controls, 20 probe sets' genes were commonly upregulated in the UCCA lines, and 108 in the sCRC lines. Five were upregulated in both UCCA and sCRC lines, and 15 and 103 only in UCCA and sCRC lines, respectively (Fig. 1b). Of the 13 known genes contained in the 15 probe sets specifically upregulated only in UCCA lines, CITED2 was upregulated with 2 independent probe sets in the same GeneChip (see Table 1 for the gene list). As we previously found that the *F. varium*-BA system induces p53-dependent cellular responses [11, 12], we focused on whether p53-signaling might be influenced. As CITED2 was identified as a CBP/p300 binding protein which regulates p53 by acetylation [18, 23, 24], we considered that CITED2 might be a candidate and subjected it to further analyses.

CITED2 acts upstream of p53

q-RT-PCR showed increased upregulation of CITED2 in UCCA cell lines as compared with sCRC cell lines on BA

Table 1 Genes upregulated by BA treatment only in the UCCA series

Probe set ID	Gene symbol	GenBank ID
237156_at	–	–
204567_s_at	ABCG1	NM_004915
210431_at	ALPPL2	J04948
200982_s_at	ANXA6	NM_001155
207980_s_at	CITED2	NM_006079
209357_at	CITED2	NM_006079
202806_at	DBN1	NM_004395
215506_s_at	DIRAS3	AK021882
211538_s_at	HSPA2	U56725
203752_s_at	JUND	NM_005354
208581_x_at	MT1X	NM_005952
201599_at	OAT	NM_000274
201364_s_at	OAZ2	AF242521
35666_at	SEMA3F	U38276
204141_at	TUBB2	NM_001069

treatment, validating the microarray results (Fig. 2a). p53 downstream molecules, $p21^{Cip1}$ and Bax, were upregulated at the mRNA level, although p53 mRNA expression was not changed (Fig. 2b). The expression of monocarboxylate transporter-1 (MCT1), a transporter of BA, was also upregulated. When an siRNA for CITED2 was introduced into UCCA24 with or without BA treatment, it significantly suppressed CITED2 mRNA expression. Although p53 mRNA expression was upregulated by knockdown of CITED2 without BA treatment, this was abrogated by BA treatment with CITED2 knockdown, indicating an upstream location of CITED2 in the p53 signaling pathway (Fig. 2c). Suppression of CITED2 expression did not significantly affect the mRNA expression of p21, Bax, and p53R2, downstream molecules of p53, with or without BA treatment. CITED2 expression was also upregulated by BA treatment at the protein level in UCCA24 after 1–12 h, with a peak at 6 h, accompanied by p53 protein accumulation and followed by p21 and Bax expression (Fig. 3). Although Bax expression was high in the non-treatment state, Bcl-2 levels were also high and decreased with BA treatment. Upregulation of CITED2 was noted within 6 h of CITED2 transfection and p53 protein accumulation was observed in parallel. Thus, on treatment with BA, the p53 protein level was upregulated without transcriptional upregulation. As p53 downstream molecules were upregulated at the mRNA and protein levels, stabilization of p53 protein without transcriptional expression could account for this discrepancy. Therefore, CITED2 could be a candidate transducer of BA responsible for post-transcriptional upregulation of p53.

BA induces apoptosis through MCT1, CITED2, and p53

As we previously reported [12], BA induced apoptosis detected by the TUNEL method in the UCCA24 line (Fig. 4a, b). Apoptosis was abundantly induced by doxorubicin with wild-type p53 as previously reported [16]. It is well known that the doxorubicin-induced apoptosis is p53-dependent [25], and apoptosis was inhibited by an siRNA for p53, but not by non-sense siRNA. BA-induced apoptosis was inhibited by 4-hydroxycinnamate (4CHC), a specific inhibitor for MCT1 in both types of cell lines, and was also significantly inhibited by siRNA for p53. CITED2 overexpression also induced apoptosis in UCCA24, and this was partially and significantly reduced by p53 siRNA, but not by non-sense siRNA. As BA activates p53 by stabilization and does not induce transcriptional expression, the partial inhibition suggests reduction of the protein pool before BA treatment or CITED2 induction. The results indicate that BA induces apoptosis through MCT1, CITED2, and p53 activation. Although the BA-induced

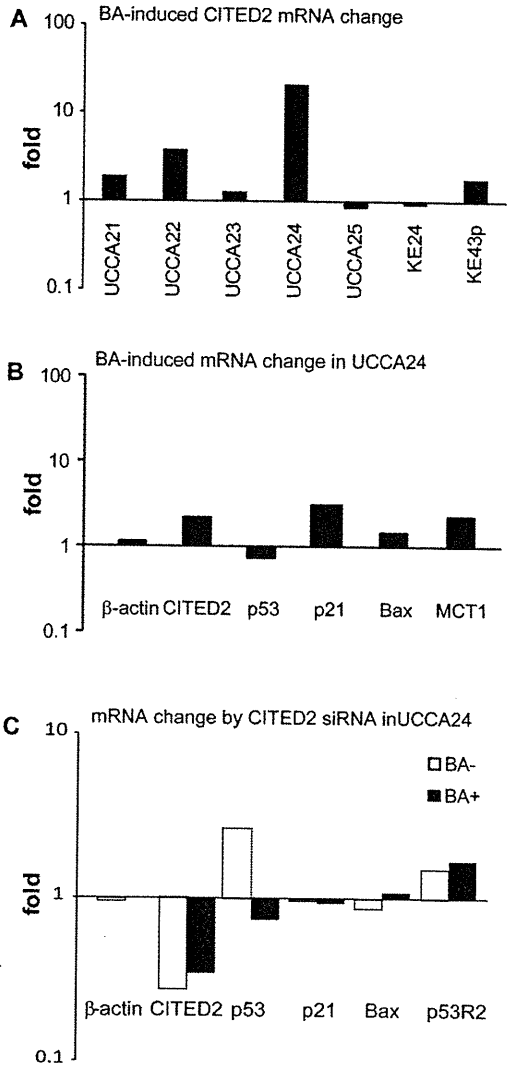

Fig. 2 q-RT-PCR for validation of CITED2 and p53-related genes, and knockdown effects of CITED2. Representative results for three independent experiments are shown. **a** CITED2 mRNA expression is induced by BA in UCCA cell lines. q-RT-PCR was performed after 2.5 mM BA was added for 24 h. UCCA cell lines, including UCCA 21 and 24 used for microarray analysis, tended to show upregulation of CITED2 mRNA expression against no BA treatment, whereas sCRC lines (KE24, KE43p) did not. **b** mRNA expression of p53-related molecules except p53 itself was increased in UCCA24 by BA treatment for 24 h, as analyzed by q-RT-PCR. Fold ratios of mRNA expression after 24 h BA treatment against no BA treatment are shown in the histogram. **c** siRNA for CITED2 was transfected 24 h before BA treatment in UCCA24. After BA treatment for 24 h, expression of β-actin, CITED2, p53, p21, Bax, and p53R2 was analyzed by q-RT-PCR. Fold expression of CITED2 siRNA transfected cells was compared with non-specific siRNA transfection. *Open* and *filled bars* show fold ratios for each gene against VIC-labeled β-actin expression with and without BA treatment

CITED2 level was almost equivalent to or greater than that in CITED2 transfected cells (Fig. 3a, b), the apoptosis level was much greater in CITED2 transfected cells (Fig. 4b).

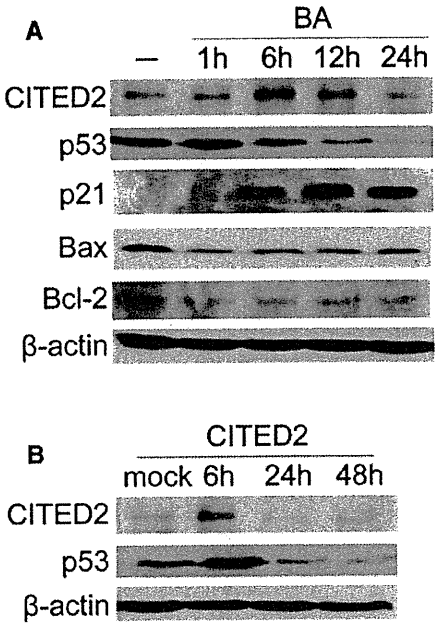

Fig. 3 CITED2, p53, and related protein expression with BA treatment and forced CITED2 expression in UCCA24. The indicated protein expression was analyzed by western blotting with BA treatment for 1, 6, 12, and 24 h (**a**) and CITED 2 transfection for 6, 24, and 48 h (**b**). CITED2 was transfected 24 h prior to BA treatment

This might be due to the direct effect of CITED2 by transfection whereas the apoptosis induced by BA could be regulated by other factors.

BA and CITED2 induce acetylation of p53 and increase protein expression

CITED2 has been identified as a co-factor for CBP/p300 [18], which induces apoptosis through acetylation of p53 [24, 26]. The amount of p53 protein was significantly increased along with the acetylated form of p53 with BA treatment (Fig. 5a) and CITED2 transfection (Fig. 5b). It is likely that CITED2 stabilizes p53 by its acetylation.

CITED2 binds to CBP/p300 in vitro

During BA treatment, we confirmed binding of CITED2 to CBP/p300 in vitro by immunoprecipitation (Fig. 5c). Binding was induced by CITED2 and CBP/p300 transfection as well as by BA treatment.

CITED2 is expressed in the surface epithelium of UC patients' colonic mucosa

Expression of CITED2 protein was evaluated in the colonic mucosa of UC patients in situ. The area (0–3) and the intensity (0–3) of CITED2 positivity were multiplied together and the correlation of the resulting CITED2 expression score with histological evidence of inflammation was assessed according to Matts (see Fig. 6a) [21]. CITED2 expression was localized in crypt bottoms of normal colonic mucosa. In contrast, it was found to be significantly increased in the surface lining epithelium and both upper and lower halves of the crypts in UC cases, whereas the increase of expression was limited to the lower halves in diverticulitis, with non-specific inflammation. In addition to the significant differences in expression score between histological grades by the Mann–Whitney's U test shown in Fig. 6b, a significant correlation of the increase of CITED2 expression with histological grade by Spearman's rank correlation test was also demonstrated, especially in lining epithelium and the upper halves of crypts ($\rho = 0.641$, $p < 0.0001$, lining epithelium, $\rho = 0.691$, $p < 0.0001$, upper crypts, $\rho = 0.460$, $p = 0.0002$, lower crypts).

Discussion

There have been many studies of the mechanisms underlying UC. Concerning roles of enterobacteria in UC development, bacterial invasion into the mucosal epithelia is considered to be associated with the production of cytokines, as a first step in inflammatory processes [10]. Thus, inflammatory cytokines produced by macrophages and lymphocytes in the stroma of the colonic mucosa are considered important factors. Interleukin-10 (IL-10)-deficient mice spontaneously develop UC-like colitis under conventional conditions, but not under specific pathogen- or germ-free conditions [6, 7]. To induce colitis in IL-10-deficient mice, commensal enteric bacteria are necessary [7]. Shkoda et al. [8] clearly revealed that IL-10 inhibits inflammation-induced endoplasmic reticulum (ER)-mediated stress responses by modulating activating transcription factor (ATF)-6 nuclear recruitment to the glucose-regulated ER stress protein-78 gene promoter in colonic epithelial cells. In inflammatory foci of UC, p53 is activated in the crypt epithelium [12], which suggests protective activity against inflammatory stress. Therefore, mutations of p53, frequently found in the early stages of UC-associated tumorigenesis, including non-tumorous regenerative mucosa, in contrast to the adenoma-carcinoma sequence [27], may greatly contribute to carcinogenesis. Short-chain fatty acids including BA are important to maintain colonic functions, and BA constitutes an energy supply for colonocytes and plays a central role in homeostasis of the colonic mucosa [28]. Previously, we detected *F. varium* by direct culture of UC patients' mucosa [14] and induced experimental UC in mice by intra-rectal administration of BA secreted from *F. varium* [9, 11]. In addition, BA induces DNA repair and apoptosis with the activation of

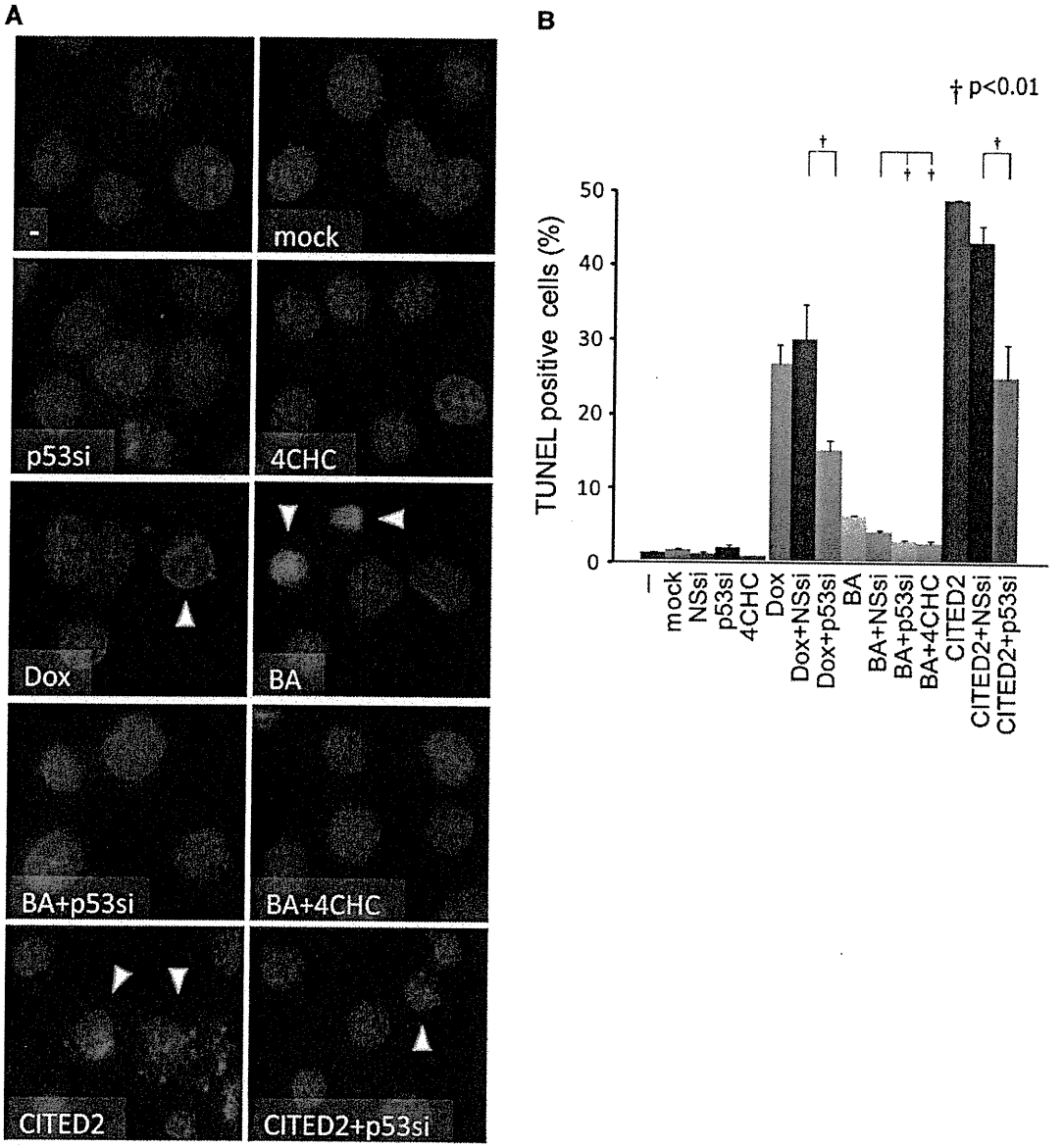

Fig. 4 Induction of p53-dependent apoptosis by BA treatment and CITED2 expression. **a** Representative images of apoptosis detected by the TUNEL method under various conditions in UCCA24 (*NT* no treatment, *Dox* treated with doxorubicin, *4CHC* treated with 4CHC, *BA* stimulated with BA, *BA + 4CHC* treated with both BA and 4CHC, *mock* mock transfection, *CITED2* CITED2 transfection). **b** Average percentages of apoptotic cells in three experiments in UCCA24 in the histogram with standard deviation bars. NSsi and p53si, siRNA for non-sense and p53 transfected, respectively. †Significant differences ($p < 0.01$) by Student's *t* test for each condition are also shown

p53–p53R2 system [12]. Therefore, BA would damage colonocytes in a high concentration condition. In order to mimic the inflammatory condition of UC in vitro, we used UCCA cell lines derived from human UC-associated adenocarcinomas [16]. Although UCCA lines are tumor cell lines and may have different characteristics from non-tumorous colonic epithelium, those used here are unique in being derived from a human UC background. As BA-induced apoptosis and activated p53-dependent DNA repair have been found in both sCRC and UCCA lines [11, 12], we here focused on their roles as a key factor for UC inflammation.

First, we established that mRNA expression of CITED2 and several other genes was upregulated by BA treatment in ulcerative colitis-associated cancer cell lines, but not in sporadic counterparts, by cDNA microarray analysis with the Percellome method [17]. Whereas two independent probe sets were listed as only upregulated in UCCA lines,

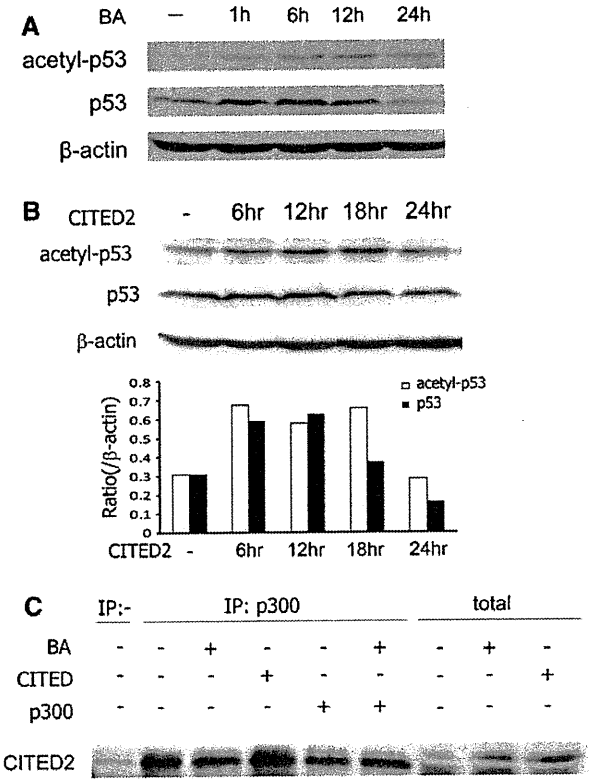

Fig. 5 Induction of p53 acetylation by BA and CITED2, accompanied by binding of CBP/p300 and CITED2 in UCCA24. **a** 2.5 mM BA treatment induced acetylation of p53 and increased the total amount of p53 from 1 to 24 h. **b** Transfection of CITED2 24 h prior to BA treatment for 24 h also induced acetylated p53 and increased the total amount of p53. A histogram of results for relative expression of acetylated p53 and p53 is shown *below*. Relative expression against *β*-actin was calculated by densitometry of western blot data. **c** Immunoprecipitation by anti-CBP/p300 antibody and immunoblotting with anti-CITED2 antibody showed binding of CITED2 and CBP/p300. *BA* indicates treatment by 2.5 mM BA for 24 h, *CITED2* and *p300* indicate the transfection of CITED2 and CBP/p300 24 h prior to the assay, respectively. A western blot from the total lysate is also illustrated

we especially focused on CITED2 among the 13 genes, because its function seemed to be closely related to p53 via CBP/p300 [18], with an upstream action. Indeed, RNAi analysis directly indicated that CITED2 is upregulated upstream of p53. Induction of CITED2 mRNA was not evident in several UCCA lines, such as UCCA23 and UCCA25 (Fig. 2). However, we confirmed the induction of CITED2 protein in those lines (data not shown) and the upregulation of CITED2 was statistically confirmed by the immunohistochemistry from the 102 inflammatory lesions of UC (Fig. 6).

Although CITED2 has been noted as an important factor for organ or tissue development [29, 30], it was originally found to inhibit the binding to hypoxia-inducible factor 1 (HIF1) [31]. Bakker et al. [32] reported CITED2 to be transcriptionally induced by FOXO3a, a member of the FOXO subfamily of Forkhead transcription factors, and to inhibit HIF1-induced apoptosis in hypoxia, which is proposed as a survival response of cancer cells. Although HIF1 induces p53-dependent apoptosis [33–35], it also causes p53-independent apoptosis via BNIP3 and NIX induction [34–36]. As Bakker et al. used p53 wild-type cell lines, it was uncertain whether CITED2 inhibited p53-dependent HIF1-induced apoptosis. In the present study, however, BA and CITED2 clearly induced apoptosis, which was inhibited by an siRNA for p53. Furthermore, the BA-induced apoptosis was inhibited by an inhibitor of MCT1, through which BA is transported into the cytoplasm [37, 38], and an siRNA for p53 partially but significantly inhibited the BA- and CITED2-induced apoptosis. Apoptosis induced by CITED2 transfection was more frequent than by BA treatment (Fig. 4b), although the BA-induced CITED2 level was almost equivalent to or greater than that in CITED2 transfected cells (Fig. 3a, b). This might be due to a direct effect of CITED2 by transfection or to apoptosis induced by BA being regulated by other factors. The dependence of BA-induced apoptosis on MCT1, demonstrated by 4CHC, an inhibitor of MCT1, should be verified by other approaches. Although protein stabilization of p53 was apparent on BA treatment with CITED2 overexpression, knockdown of p53 at the mRNA level could also inhibit the BA–CITED2 pathway. Therefore, CITED2 possibly plays different roles in BA-induced and HIF1-induced apoptosis, which might depend on modulation of the phosphorylation or acetylation sites of p53.

According to recent studies, p53 induces apoptosis via acetylation of lysine 120 on DNA damage or in response to stress signaling with CBP/p300 binding [24, 26]. The acetylated form of p53 is stable with regard to the Mdm2-ubiquitination system [39]. We here demonstrated acetylation of p53 by BA treatment and forced CITED2 expression accompanied by p53 protein accumulation (Fig. 5a, b). At the same time, binding of the CITED2 and CBP/p300 was also observed by immunoprecipitation (Fig. 5c). Therefore, we conclude that CITED2 is upregulated by BA, in turn activating p53-dependent apoptosis via acetylation of p53 protein (Fig. 7). Although transcription of p53 was not observed, the data support p53 protein stabilization by BA and CITED2. Further investigation of the half-life of p53 after BA treatment with or without CITED2 knockdown should clarify this point.

In UC, p53 gene alteration is observed even in non-tumorous regenerative epithelium [27]. In addition, p53 expression is upregulated in inflammatory foci of UC without gene mutation and the p53 and p53R2 DNA repair system is accelerated [12]. Therefore, the repair capacity may be overloaded in active UC. We previously found greater upregulation of Bax protein in UCCA as compared

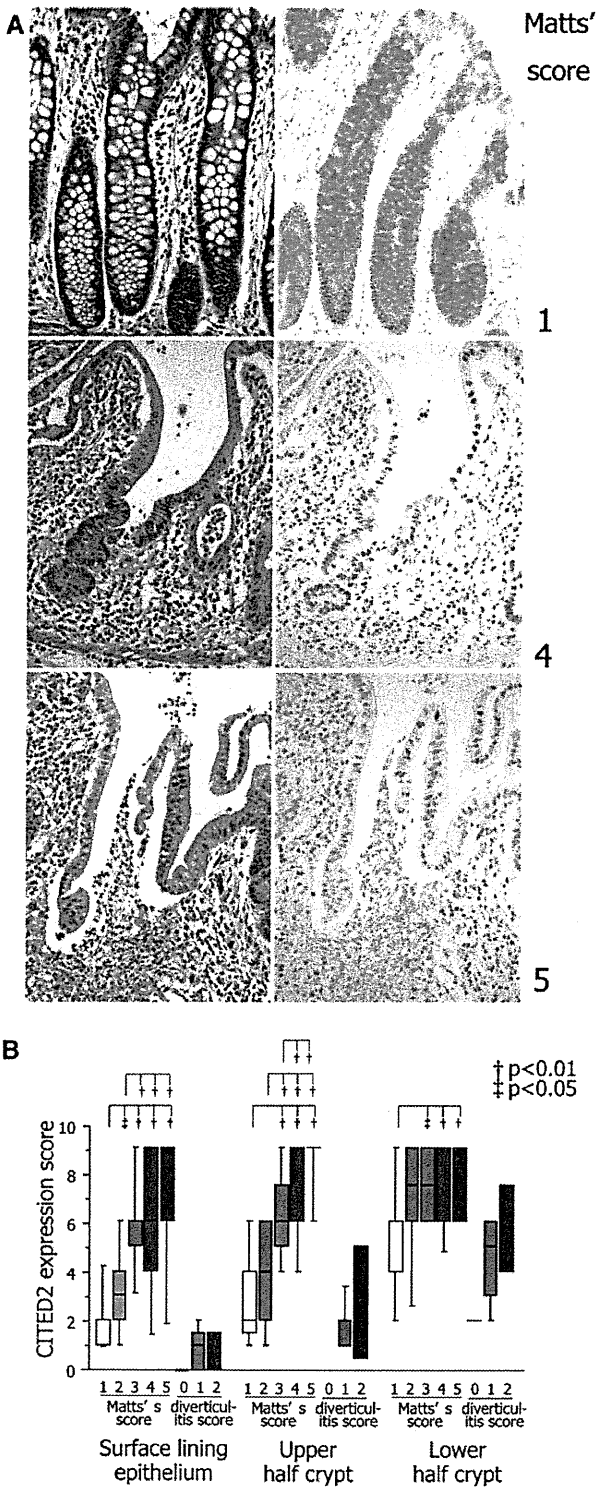

◀ **Fig. 6** CITED2 expression in inflammatory foci of ulcerative colitis. **a** Immunohistochemical staining of CITED2 is shown in the *right panels* and semi-serial H&E sections are shown in the *left panels*. Examples of inactive UC (Matts' score 1, *upper panel*) and active UC (Matts' score 4 and 5, *middle* and *lower panel*) are presented. Strong CITED2 expression is remarkable in epithelial nuclei in active UC. **b** CITED2 expression correlates with activity of inflammation of UC in situ. The area (0–3) and the intensity (0–3) of CITED2 expression were evaluated and the CITED2 expression score (0–9) was calculated by multiplying the two results. The inflammatory grade of the diverticulosis cases was scored from 0 to 2 (none, mild, severe). The CITED2 expression scores are shown along with histological scores. Median values are shown by the *horizontal line*, the *box* represents values between the 25th and 75th percentiles, and the *lower* and *upper bars* indicate the 10th and 90th percentiles, respectively. $^{\dagger}p < 0.01$ and $^{\ddagger}p < 0.05$ by Mann–Whitney's *U* test

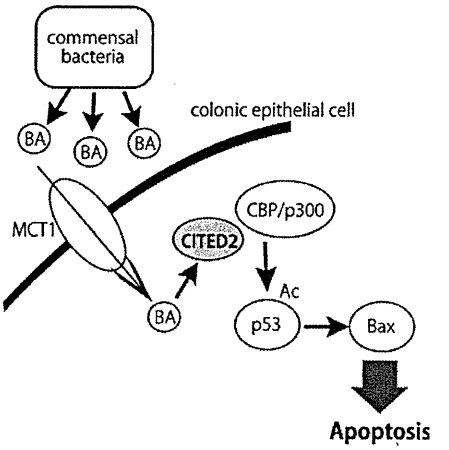

Fig. 7 Scheme for BA-induced apoptosis. BA produced by commensal bacteria, such as *F. varium*, is incorporated by MCT1 and induces CITED2 expression. The CITED2-CBP/p300 complex then acetylates p53 which stabilizes the protein, resulting in upregulated transcription of proapoptotic genes including Bax, and induction of apoptosis. Apoptosis of colonic epithelial cells leads to erosion of the mucosa, so that bacteria can more easily colonize. *Ac* acetylation; *BA* butyric acid; *MCT1* monocarboxylate transporter-1

with sCRC [40], which might have a similar effect. Matts' histological scores based on the infiltration of neutrophils and the presence of cryptitis, crypt abscess and erosion, reflect the inflammation activity of UC [21]. The fact that CITED2 expression in UC is also increased in the upper halves of the crypts and positively correlated with the histological activity of UC, evaluated by Matts' histological scores, is clear evidence of an association with UC inflammation. In contrast, although the CITED2 expression was increased in the inflammatory foci of diverticulitis, the expression score was almost at the same level as that of the inactive UC (Matts' score 1). This might indicate that the BA-CITED2 system is specifically involved in the UC inflammation, and not under conditions of non-specific colonic inflammation such as diverticulitis.

Previously, we showed that specific enterobacteria including *F. varium* are frequently detectable in UC patients' mucosa. Here we showed BA-induced apoptosis via CITED2 induction and p53 activation, and that CITED2 expression clearly correlates with histological UC

activity. Although the reported role of CITED2 in hypoxic stress does not coincide with our present results [32], our present histopathological study supports a scenario in human UC involving another CITED2-activating pathway. Thus, highly concentrated BA produced by enteric bacteria would induce CITED2-p53-dependent apoptosis in the colonic epithelium and cause erosion, which is typical of active UC. With mucosal erosion, enteric bacteria can easily infiltrate into the colonic stroma and stimulate macrophages [41], which would enhance inflammation by producing inflammatory cytokines. Apoptosis induced by BA was here inhibited by an siRNA for p53, as well as by 4CHC, an inhibitor of MCT1 (Fig. 4b), which suggests the possibility of anti-inflammation targeted therapy. However, mechanisms of UC generation still need further analysis, particular with regard to enteric bacteria. In conclusion, we propose that p53 activation via CITED2 upregulation by BA and consequent p53 acetylation is a possible mechanism underlying UC development.

Acknowledgments The authors appreciate the technical assistance of Ms. Y. Numata and would like to thank Dr. M. Moore for revising the English of the manuscript. This work was supported in part by Grants-in-Aid for Scientific Research from the Japan Society for the Promotion of Science, Health Sciences Research Grants H18-Kagaku-Ippan-001 from the Ministry of Health, Labour and Welfare, Japan, Grants-in-Aid from Kitasato University Graduate School of Medical Sciences and Kanagawa Nanbyo Foundation.

Conflicts of interest The authors disclose no conflicts with this work.

References

1. Arai N, Mitomi H, Ohtani Y, Igarashi M, Kakita A, Okayasu I. Enhanced epithelial cell turnover associated with p53 accumulation and high p21WAF1/CIP1 expression in ulcerative colitis. Mod Pathol. 1999;12:604–11.
2. Mitsuhashi J, Mikami T, Saigenji K, Okayasu I. Significant correlation of morphological remodeling in ulcerative colitis with disease duration and between elevated p53 and p21 expression in rectal mucosa and neoplastic development. Pathol Int. 2005;55:113–21.
3. Okayasu I, Hatakeyama S, Yamada M, Ohkusa T, Inagaki Y, Nakaya R. A novel method in the induction of reliable experimental acute and chronic ulcerative colitis in mice. Gastroenterology. 1990;98:694–702.
4. Okayasu I, Ohkusa T, Kajiura K, Kanno J, Sakamoto S. Promotion of colorectal neoplasia in experimental murine ulcerative colitis. Gut. 1996;39:87–92.
5. Okayasu I, Yamada M, Mikami T, Yoshida T, Kanno J, Ohkusa T. Dysplasia and carcinoma development in a repeated dextran sulfate sodium-induced colitis model. J Gastroenterol Hepatol. 2002;17:1078–83.
6. Kuhn R, Lohler J, Rennick D, Rajewsky K, Muller W. Interleukin-10-deficient mice develop chronic enterocolitis. Cell. 1993;75:263–74.
7. Sellon RK, Tonkonogy S, Schultz M, Dieleman LA, Grenther W, Balish E, et al. Resident enteric bacteria are necessary for development of spontaneous colitis and immune system activation in interleukin-10-deficient mice. Infect Immun. 1998;66:5224–31.
8. Shkoda A, Ruiz PA, Daniel H, Kim SC, Rogler G, Sartor RB, et al. Interleukin-10 blocked endoplasmic reticulum stress in intestinal epithelial cells: impact on chronic inflammation. Gastroenterology. 2007;132:190–207.
9. Ohkusa T, Sato N, Ogihara T, Morita K, Ogawa M, Okayasu I. *Fusobacterium varium* localized in the colonic mucosa of patients with ulcerative colitis stimulates species-specific antibody. J Gastroenterol Hepatol. 2002;17:849–53.
10. Ohkusa T, Yoshida T, Sato N, Watanabe S, Tajiri H, Okayasu I. Commensal bacteria can enter colonic epithelial cells and induce proinflammatory cytokine secretion: a possible pathogenic mechanism of ulcerative colitis. J Med Microbiol. 2009;58:535–45.
11. Ohkusa T, Okayasu I, Ogihara T, Morita K, Ogawa M, Sato N. Induction of experimental ulcerative colitis by *Fusobacterium varium* isolated from colonic mucosa of patients with ulcerative colitis. Gut. 2003;52:79–83.
12. Yoshida T, Haga S, Numata Y, Yamashita K, Mikami T, Ogawa T, et al. Disruption of the p53–p53r2 DNA repair system in ulcerative colitis contributes to colon tumorigenesis. Int J Cancer. 2006;118:1395–403.
13. Ohkusa T, Nomura T, Terai T, Miwa H, Kobayashi O, Hojo M, et al. Effectiveness of antibiotic combination therapy in patients with active ulcerative colitis: a randomized, controlled pilot trial with long-term follow-up. Scand J Gastroenterol. 2005;40:1334–42.
14. Nomura T, Ohkusa T, Okayasu I, Yoshida T, Sakamoto M, Hayashi H, et al. Mucosa-associated bacteria in ulcerative colitis before and after antibiotic combination therapy. Aliment Pharmacol Ther. 2005;21:1017–27.
15. Ohkusa T, Kato K, Terao S, Chiba T, Mabe K, Murakami K, et al. Newly developed antibiotic combination therapy for ulcerative colitis: a double-blind placebo-controlled multicenter trial. Am J Gastroenterol. 2010;105:1820–9.
16. Yamashita K, Yasuda S, Kuba T, Otani Y, Fujiwara M, Okayasu I. Unique characteristics of rectal carcinoma cell lines derived from invasive carcinomas in ulcerative colitis patients. Cancer Sci. 2004;95:211–7.
17. Kanno J, Aisaki K, Igarashi K, Nakatsu N, Ono A, Kodama Y, et al. "Per cell" normalization method for mRNA measurement by quantitative PCR and microarrays. BMC Genomics. 2006;7:64.
18. Leung MK, Jones T, Michels CL, Livingston DM, Bhattacharya S. Molecular cloning and chromosomal localization of the human CITED2 gene encoding p35srj/Mrg1. Genomics. 1999;61:307–13.
19. Sanosaka T, Namihira M, Asano H, Kohyama J, Aisaki K, Igarashi K, et al. Identification of genes that restrict astrocyte differentiation of midgestational neural precursor cells. Neuroscience. 2008;155:780–8.
20. Aisaki K, Aizawa S, Fujii H, Kanno J, Kanno H. Glycolytic inhibition by mutation of pyruvate kinase gene increases oxidative stress and causes apoptosis of a pyruvate kinase deficient cell line. Exp Hematol. 2007;35:1190–200.
21. Matts SG. The value of rectal biopsy in the diagnosis of ulcerative colitis. Q J Med. 1961;30:393–407.
22. Sinicrope FA, Lemoine M, Xi L, Lynch PM, Cleary KR, Shen Y, et al. Reduced expression of cyclooxygenase 2 proteins in hereditary nonpolyposis colorectal cancers relative to sporadic cancers. Gastroenterology. 1999;117:350–8.
23. Braganca J, Eloranta JJ, Bamforth SD, Ibbitt JC, Hurst HC, Bhattacharya S. Physical and functional interactions among AP-2 transcription factors, p300/CREB-binding protein, and CITED2. J Biol Chem. 2003;278:16021–9.

24. Kruse JP, Gu W. Modes of p53 regulation. Cell. 2009;137: 609–22.
25. Lowe SW, Ruley HE, Jacks T, Housman DE. p53-dependent apoptosis modulates the cytotoxicity of anticancer agents. Cell. 1993;74:957–67.
26. Vousden KH, Prives C. Blinded by the light: the growing complexity of p53. Cell. 2009;137:413–31.
27. Yoshida T, Mikami T, Mitomi H, Okayasu I. Diverse p53 alterations in ulcerative colitis-associated low-grade dysplasia: full-length gene sequencing in microdissected single crypts. J Pathol. 2003;199:166–75.
28. Scheppach W. Effects of short chain fatty acids on gut morphology and function. Gut. 1994;35:S35–8.
29. Sperling S, Grimm CH, Dunkel I, Mebus S, Sperling HP, Ebner A, et al. Identification and functional analysis of CITED2 mutations in patients with congenital heart defects. Hum Mutat. 2005;26:575–82.
30. Qu X, Lam E, Doughman YQ, Chen Y, Chou YT, Lam M, et al. Cited2, a coactivator of HNF4alpha, is essential for liver development. EMBO J. 2007;26:4445–56.
31. Bhattacharya S, Michels CL, Leung MK, Arany ZP, Kung AL, Livingston DM. Functional role of p35srj, a novel p300/CBP binding protein, during transactivation by HIF-1. Genes Dev. 1999;13:64–75.
32. Bakker WJ, Harris IS, Mak TW. FOXO3a is activated in response to hypoxic stress and inhibits HIF1-induced apoptosis via regulation of CITED2. Mol Cell. 2007;28:941–53.
33. Suzuki H, Tomida A, Tsuruo T. Dephosphorylated hypoxia-inducible factor 1alpha as a mediator of p53-dependent apoptosis during hypoxia. Oncogene. 2001;20:5779–88.
34. Harris AL. Hypoxia—a key regulatory factor in tumour growth. Nat Rev Cancer. 2002;2:38–47.
35. Greijer AE, van der Wall E. The role of hypoxia inducible factor 1 (HIF-1) in hypoxia induced apoptosis. J Clin Pathol. 2004;57: 1009–14.
36. Sowter HM, Ratcliffe PJ, Watson P, Greenberg AH, Harris AL. HIF-1-dependent regulation of hypoxic induction of the cell death factors BNIP3 and NIX in human tumors. Cancer Res. 2001; 61:6669–73.
37. Garcia CK, Li X, Luna J, Francke U. cDNA cloning of the human monocarboxylate transporter 1 and chromosomal localization of the SLC16A1 locus to 1p13.2–p12. Genomics. 1994;23:500–3.
38. Cuff M, Dyer J, Jones M, Shirazi-Beechey S. The human colonic monocarboxylate transporter Isoform 1: its potential importance to colonic tissue homeostasis. Gastroenterology. 2005;128:676–86.
39. Gu W, Roeder RG. Activation of p53 sequence-specific DNA binding by acetylation of the p53 C-terminal domain. Cell. 1997;90:595–606.
40. Yoshida T, Matsumoto N, Mikami T, Okayasu I. Upregulation of p16(INK4A) and Bax in p53 wild/p53-overexpressing crypts in ulcerative colitis-associated tumours. Br J Cancer. 2004;91: 1081–8.
41. Ohkusa T, Okayasu I, Tokoi S, Ozaki Y. Bacterial invasion into the colonic mucosa in ulcerative colitis. J Gastroenterol Hepatol. 1993;8:116–8.

The Journal of Toxicological Sciences (J. Toxicol. Sci.)
Vol.37, No.2, 373-380, 2012

Original Article

Development of humanized steroid and xenobiotic receptor mouse by homologous knock-in of the human steroid and xenobiotic receptor ligand binding domain sequence

Katsuhide Igarashi[1], Satoshi Kitajima[1], Ken-ichi Aisaki[1], Kentaro Tanemura[1], Yuhji Taquahashi[1], Noriko Moriyama[1], Eriko Ikeno[1], Nae Matsuda[1], Yumiko Saga[2,3], Bruce Blumberg[4] and Jun Kanno[1]

[1]Division of Cellular and Molecular Toxicology, Biological Safety Research Center, National Institute of Health Sciences, 1-18-1 Kamiyoga, Setagaya-ku, Tokyo, 158-8501, Japan
[2]Division of Mammalian Development, National Institute of Genetics, Yata 1111, Mishima 411-8540, Japan
[3]The Graduate University for Advanced Studies (Sokendai), Yata 1111, Mishima 411-8540, Japan
[4]Department of Developmental and Cell Biology, 2011 Biological Sciences 3, University of California, Irvine, CA 92697-2300, USA

(Received December 7, 2011; Accepted January 12, 2012)

ABSTRACT — The human steroid and xenobiotic receptor (SXR), (also known as pregnane X receptor PXR, and NR1I2) is a low affinity sensor that responds to a variety of endobiotic, nutritional and xenobiotic ligands. SXR activates transcription of Cytochrome P450, family 3, subfamily A (CYP3A) and other important metabolic enzymes to up-regulate catabolic pathways mediating xenobiotic elimination. One key feature that demarcates SXR from other nuclear receptors is that the human and rodent orthologues exhibit different ligand preference for a subset of toxicologically important chemicals. This difference leads to a profound problem for rodent studies to predict toxicity in humans. The objective of this study is to generate a new humanized mouse line, which responds systemically to human-specific ligands in order to better predict systemic toxicity in humans. For this purpose, the ligand binding domain (LBD) of the human SXR was homologously knocked-in to the murine gene replacing the endogenous LBD. The LBD-humanized chimeric gene was expressed in all ten organs examined, including liver, small intestine, stomach, kidney and lung in a pattern similar to the endogenous gene expressed in the wild-type (WT) mouse. Quantitative reverse transcription-polymerase chain reaction (RT-PCR) analysis showed that the human-selective ligand, rifampicin induced Cyp3a11 and Carboxylesterase 6 (Ces6) mRNA expression in liver and intestine, whereas the murine-selective ligand, pregnenolone-16-carbonitrile did not. This new humanized mouse line should provide a useful tool for assessing whole body toxicity, whether acute, chronic or developmental, induced by human selective ligands themselves and subsequently generated metabolites that can trigger further toxic responses mediated secondarily by other receptors distributed body-wide.

Key words: Steroid and xenobiotic receptor, Pregnane X receptor, Humanized mouse, Ligand binding domain, Knock-in mouse

INTRODUCTION

Most orally administered xenobiotics are metabolized first by the intestine and then by the liver after portal transport. The expression levels of enzymes involved in xenobiotic metabolism are regulated at the transcriptional level by key xenobiotic sensors including the steroid and xenobiotic receptor (SXR), also known as the pregnane X receptor (PXR), pregnane activated receptor (PAR) and NR1I2 (Bertilsson *et al.*, 1998; Lehmann *et al.*, 1998; Blumberg *et al.*, 1998). SXR is important in the field of toxicology for at least two reasons. Firstly, this receptor system induces the expression of CYP3A and CYP2B enzymes, the major metabolizers of pharmaceu-

Correspondence: Jun Kanno (E-mail: kanno@nihs.go.jp)

ticals and xenobiotics. Therefore, SXR is a key mediator of drug- and chemical-induced toxicity as well as drug-drug and drug-nutrient interactions (Zhou *et al.*, 2004). Secondly, the orthologous rodent and human receptors exhibit differential sensitivity for a subset of chemical ligands important in the field of toxicology. For example, rifampicin (RIF) is a specific and selective activator of human SXR, whereas pregnenolone 16a-carbonitrile (PCN) is selective for the rodent orthologue.

Rodent-human differences in CYP3A and CYP2B-mediated responses to xenobiotics can be a profound problem in toxicologic studies where rodents are used to predict the toxicity of a compound in humans (Ma *et al.*, 2007). Therefore, development of a murine model that reconstructs the SXR-mediated systemic response of humans is of a great significance in toxicology.

Human and rodent SXRs share ~95% amino acid sequence identity in the DNA-binding domain (DBD) but only about 77% identity in the LBD. Tirona *et al.* (2004) analyzed the ligand selectivity of a human-rat chimeric protein and showed that the species differences are primarily defined by sequence differences in the LBD. Watkins and colleagues showed that the key residues responsible for the majority of the ligand selectivity were Leu 308 (human) and Phe305 (rat and mouse). Crystallographic analysis located these amino acids within or neighboring the flexible loop that forms a part of the pore to the ligand-binding cavity. Swapping the rodent and human-specific residues was shown to modulate the activation by the human-selective activator RIF *in vitro* (Watkins *et al.*, 2001). According to those findings, a simple replacement of the mouse LBD with the human sequence should be sufficient to "humanize" the ligand binding properties as well as activation of the downstream target genes.

Three kinds of humanized mice have already been generated. One is the SXR-null/Alb-SXR mouse (Alb-SXR mouse) made by crossing the SXR knockout mice with a transgenic mouse line that expresses human SXR in liver under the control of the albumin promoter (Xie *et al.*, 2000). Gonzalez and colleagues generated a transgenic mouse expressing a human BAC containing the entire hSXR gene in a SXR null background, thus controlled under human SXR promoter (SXR BAC mouse) (Ma *et al.*, 2007). Another mouse is the human SXR genome knock-in mice (hSXR genome mouse) (Scheer *et al.*, 2008). The human SXR genomic region from exon 2 to exon 9 was knocked-in to mouse SXR exon 2. This mouse expresses the human full length SXR mRNA under the control of mouse SXR promoter regulation. Although useful for toxicology studies, these mice have disadvantages in that the human SXR is expressed only in the liver (Alb-SXR mouse), hSXR mRNA is not expressed in all of the tissues where SXR is known to be expressed (SXR BAC mouse), and there might be potential differences in the binding affinities of hSXR DNA-binding domain (DBD) to *cis*-acting elements in mouse SXR target genes (hSXR genome mouse).

As noted above, it is known that the critical differences between human and rodent ligand-selectivity reside in the LBD. Therefore, when our project to generate a humanized SXR mouse was initiated, we reasoned that altering the LBD would be sufficient to generate a humanized ligand selectivity. We decided to retain the mouse DBD to avoid any potential differences between the binding affinities of the chimeric receptor for cis-acting elements in the mouse genome. To maintain the tissue-specific expression pattern of the endogenous gene, we inserted the human cDNA encoding the region carboxyl-terminal to the DBD into the mouse gene. This retains all of the 5' and 3' regulatory elements in the mouse gene, as well as introns 1 and 2, which contain important elements for regulating SXR expression (Jung *et al.*, 2006).

Here we report a new line of mouse (hSXRki mouse) in which a cDNA encoding the human LBD is homologously recombined into the mouse gene after exon 3. The tissue distribution of the resulting chimeric mouse DBD-human LBD mRNA is comparable to that of the WT mouse. The hSXRki mouse showed a fully humanized response to the human-selective activator RIF in that the Cyp3a11 mRNA was induced in liver and mucosa of small intestine in response to RIF, but not the rodent-selective compound PCN. This new mouse line should provide a useful tool for assessing the whole body toxicity induced by a human selective SXR ligand itself and its subsequently generated metabolite(s) that can trigger further toxic responses through other pathways body-wide.

MATERIALS AND METHODS

Generation of hSXRki knock-in mice

A DNA fragment of mouse SXR intron 2 to exon 3 was PCR amplified using mouse BAC DNA (BAC clone No. RP23-351P21) as a template. Primers used were BAC39486FW and mSXR462RV (for sequences of the primers see Table1). This fragment was connected to the LBD of human SXR cDNA from amino acid 105 through the carboxyl terminus amplified by the PCR primers: hSXR904FW and hSXR1887RVEcoRI (template; human SXR cDNA). The 3'UTR of bovine growth hormone (BGH) was added to 3' to the terminal codon. This concatenated fragment was introduced to a vector, which

Table 1. List of primer pairs

Purpose	Primer name	Sequence (5' to 3')
Targeting vector construction	BAC39486FW	CCATGGGTACCACGAATAACAA
	mSXR462RV	CATGCCACTCTCCAGGCA
	hSXR904FW	AAGAAGGAGATGATCATGTCCG
	hSXR1887RVEcoRI	CCGAATTCTCATCATCAGCTACCTGTGATACCGAACA
Genotyping	NeoAL2	GGGGATGCGGTGGGCTCTATGGCTT
	SXR RC RV5	TGAGAGTGCACAAGTTCAAGCT
	WTInt5	AGTGATGGGAACCACTCCTG
	WTEx6RV	TGGTCCTCAATAGGCAGGTC
	mhSXRE4	GTGAACGGACAGGGACTCAG
	mhSXRSARV	CTCTCCTGGCTCATCCTCAC
Percellome quantitative RT-PCR	Cyp3a11 FW	CAGCTTGGTGCTCCTCTACC
	Cyp3a11 RV	TCAAACAACCCCCATGTTTT
	Ces6 FW	GGAGCCTGAGTTCAGGACAGAC
	Ces6 RV	ACCCTCACTGTTGGGGTTC
	mouse SXR FW	AATCATGAAAGACAGGGTTC
	mouse SXR RV	AAGAGCACAGATCTTTCCG
	human SXR FW	ATCACCCGGAAGACACGAC
	human SXR RV	AAGAGCACAGATCTTTCCG
	mouse-human SXR FW	CCCATCAACGTAGAGGAGGA

has the neomycin resistance gene with loxP sequence at both ends, removable with Cre recombinase (Saga *et al.*, 1999). A 7kb KpnI fragment containing intron 2 was used as a long arm and 1.3kb PstI-EcoRI fragment containing from exon 8 to intron 8 was used as a short arm for homologous recombination (Fig. 1). The resulting targeting vector was linearized with SacII and introduced by electroporation to TT2 ES cell line (Yagi *et al.*, 1993) and neomycin resistant clones were selected, PCR genotyped, and confirmed by the Southern blotting. For generation of chimeric mice, these ES clones were aggregated with ICR 8-cell embryos and transferred to pseudopregnant female recipients. The chimeric mice born were bred with ICR females. Germ line transmission of the targeted allele was confirmed by PCR. A mouse was crossed with a CAG-Cre transgenic mouse (Sakai and Miyazaki, 1997) to evict the neomycin resistance gene, and back crossed to C57BL/6 CrSlc (SLC, Inc., Shizuoka, Japan) at least 6 generations and used for the analysis.

PCR Genotyping (See Table 1 for primer sequences)

Primers for identification of homologously recombined ES clones were NeoAL2 and SXR RC RV5. DNA purified from the tail of each mouse was used for PCR genotying. Primers for WT detection were WTInt5 and WTEx6RV amplifying a product of 755 bp. Primers for confirmation of removal of the neomycin resistance gene were mhSXRE4 and mhSXRSARV amplifying a product of 1,223 bp.

Southern blot analysis

To confirm homologous recombination, DNA from ES cell cultures was purified and digested with BamHI and XhoI, then electrophoresed and analyzed by Southern hybridization (Saga *et al.*, 1997). Mouse SXR exon 9 region which remains after homologous recombination was used for the probe. The restriction fragments from the WT allele and targeted allele are 2,305 bp and 1,925 bp, respectively.

Chemicals

RIF (molecular weight 822.95) and PCN (molecular weight 341.49) were purchased from Sigma-Aldrich (St. Louis, MO, USA). Corn oil was purchased from Wako Pure Chemical Industries (Osaka, Japan).

Quantitative RT-PCR (Percellome PCR) (See Table 1 for primer sequences)

The method for Percellome quantitative RT-PCR was described previously (Kanno *et al.*, 2006). Briefly, tissue pieces stored in RNAlater (Ambion, Austin, TX, USA) were homogenized and lysed in RLT buffer (Qiagen GmbH., Germany) and 10 μl aliquots were used

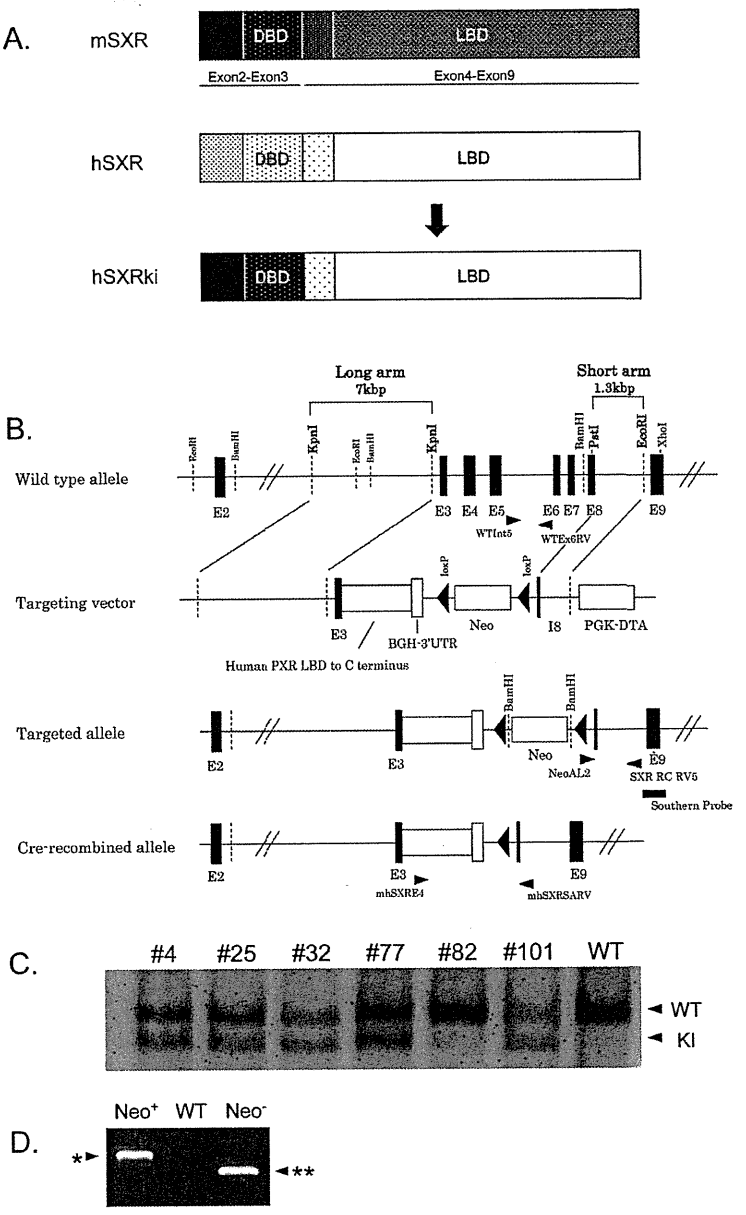

Fig. 1. Targeting strategy used to generate the hSXRki mouse. A) Diagram of hSXRki chimeric protein. Hinge region and ligand binding domain (LBD) of human SXR are knocked-in to mouse SXR, resulting in chimeric protein having murine N-ternial domain and DNA binding domain (DBD). B) Targeting strategy used to generate the hSXRki mouse. The chimeric mouse DBD and human LBD fragment, followed by the BGH 3' UTR were knocked-in to the mouse SXR gene. The genomic region spanning from exon 3 to exon 8 was substituted by the inserted fragment with the remainder of the gene remaining intact. C) Confirmation of homologous recombination by southern blot analysis. Six ES clones positive for recombination by PCR genotyping were further analyzed by southern blot (clones #4 ~ #101). Lower bands (1925 bp) indicate successful homologous recombination; upper bands (2305 bp) correspond to WT allele. Clones #4, #25, #32, #77 and #101 were confirmed as homologous recombinants; clones #4 and #25 were used for the generation of chimeric mice. D) Confirmation of Cre-mediated removal of the neomycin resistance gene. Mouse tail genome DNA was PCR amplified with the primer set, mhSXRE4 and mhSXRSARV. *: 2,858 bp (for the mice having the neomycin resistance gene), **: 1,223 bp (for the mice without the neomycin resistance gene).

for genomic DNA quantification with PicoGreen fluorescent dye (Invitrogen, Carlsbad, CA, USA). A prepared spike mRNA cocktail solution containing known quantity of five mRNAs of bacillus subtilis was added to the tissue lysate in proportion to the DNA quantity. Total RNA was purified from the lysate using the RNeasy kit (Qiagen). One microgram of total RNA was reverse-transcribed with SuperScript II (Invitrogen). Quantitative real time PCR was performed with an ABI PRISM 7900 HT sequence detection system (Applied Biosystems) using SYBR Green PCR Master Mix (Applied Biosystems), with initial denaturation at 95°C for 10 min followed by 40 cycles of 30 sec at 95°C and 30 sec at 60°C and 30 sec at 72°C, and Ct values were obtained. Primers for Cyp3a11 were Cyp3a11 FW and Cyp3a11 RV. Primers for Ces6 were Ces6 FW and Ces6 RV. Primers for mouse SXR selective quantification were mouse SXR FW and mouse SXR RV. Primers for hSXRki selective quantification were human SXR FW and human SXR RV. Primers for both mouse SXR and hSXRki quantification were mouse-human SXR FW and mouse-human SXR RV that amplify the DBD region of the chimera.

In Situ Hybridization analysis

Digoxigein-labeled cRNA probe for Cyp3a11 was synthesized according to Suzuki *et al.* (2005) by RT-PCR using mouse liver cDNA as a template. The primers used were as follows: forward 5'-GATTGGTTTTGATGCCTGGT-3' and reverse 5'-CAAGAGCTCACATTTTTCATCA-3'. The amplified product was sequence confirmed and ligated with Block-iT T7-TOPO (Invitrogen) Linker, which contains the T7 promoter site. A secondary PCR was performed to generate the sense and antisense DNA templates. For antisense template, Block-iT T7 Primer and Cyp3a11 forward primer (or reverse primer for generation of sense DNA template), the same primer as for the first PCR amplification, were used. With these DNA templates, both sense and antisense digoxigenin-labeled riboprobes were synthesized using a DIG RNA labeling kit (Roche Diagnostics, Germany) according to the manufacturer's protocol.

ISH on paraffin sections was carried out according to Suzuki *et al.* with a modification; permeabilization condition 98°C for 15 min in HistoVT One (Nacalai tesque, Japan).

Animals experiments

Male hSXRki and WT mice were maintained under a 12 hr light/12 hr dark cycle with water and chow (CRF-1, Oriental Yeast Co. Ltd., Tokyo, Japan) provided *ad libitum*. The animal studies were conducted in accordance with the Guidance for Animal Studies of the National Institute of Health Sciences under Institutional approval. The expression level of the hSXRki and WT SXR mRNA of ten organs (brain, thymus, heart, lung, liver, stomach, spleen, kidney, small intestine and testis) were analyzed on 15 weeks old male mice (n = 2) by the Percellome quantitative RT-PCR.

For the demonstration of selective gene induction by RIF and PCN in hSXRki and WT male mice on 13 weeks

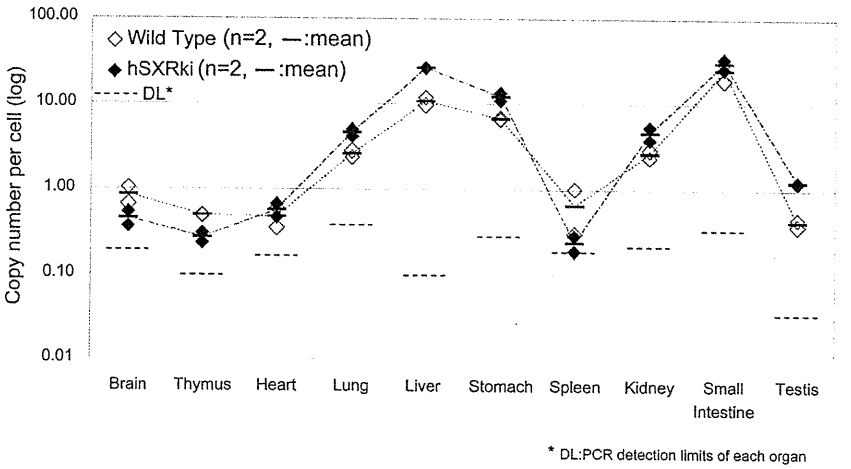

Fig. 2. Conservation of tissue expression patterns of hSXRki mRNA in the knock-in mouse. Percellome quantitative RT-PCR analysis was performed to measure the absolute expression levels of WT SXR mRNA and hSXRki mRNA in ten organs of WT and hSXRki mice. The expression levels of hSXRki mRNA among organs were comparable to WT.

old, three mice per group were singly dosed orally with vehicle (corn oil+0.1% DMSO), 10, 30, or 100 mg/kg of RIF, or 20, 70, or 200 mg/kg PCN (approximately equivalent in molar dose). Eight hours later, mice were sacrificed by exsanguination under ether anesthesia and the liver and the small intestine mucosa were sampled. Liver samples in small pieces were stored in RNA later (Applied Biosystems, Foster City, CA, USA) for further analysis. The small intestine under ice-cooled condition was longitudinally opened, gently rinsed with RNase-free saline and the epithelium was scraped with a glass slide and immersed in RNAlater. For *in situ* hybridization (ISH) of Cyp3a11 in the liver, 15 weeks old male hSXRki and WT mice were dosed orally with vehicle (corn oil), RIF (10 mg/kg), or PCN (40 mg/kg) daily for 3 days and liver sampled 24 hr later. All mice were sacrificed by exsanguination under ether anesthesia.

Statistical analysis

All values are expressed as the means ± S.D. and group differences analyzed by unpaired Student's *t* test or one-way ANOVA followed by Dunnett's post hoc comparison. Level of significance was set at $p < 0.05$.

RESULTS

Generation of hSXRki knock-In mice

Among 144 neomycin resistant TT2 ES clones, six PCR positive clones were further submitted to Southern blotting for the confirmation of homologous recombination. As shown in Fig. 1C, five clones were confirmed, and two (#4 and #25) were used to generate chimeric mice. The resulting mice were backcrossed to ICR strain to confirm germline transmission. One clone (#4) was crossed to a mouse constitutively expressing Cre recombinase to remove the neomycin resistance gene (Fig. 1D) and backcrossed to C57BL/6 CrSlc for at least 6 generations before further analysis.

Tissue distribution of hSXRki mRNA

Ten tissues, i.e., brain, thymus, heart, lung, liver, stomach, spleen, kidney, small intestine and testis from both hSXRki and WT mice were measured for hSXRki or WT SXR mRNA expression by the Percellome quantitative RT-PCR. As shown in Fig. 2, the levels of hSXRki mRNA are comparable to that of SXR in WT mouse and expressed in all tissues analyzed.

Humanized responses in hSXRki mouse

Humanized response of hSXRki was demonstrated by administration of the mouse-specific ligand PCN and the

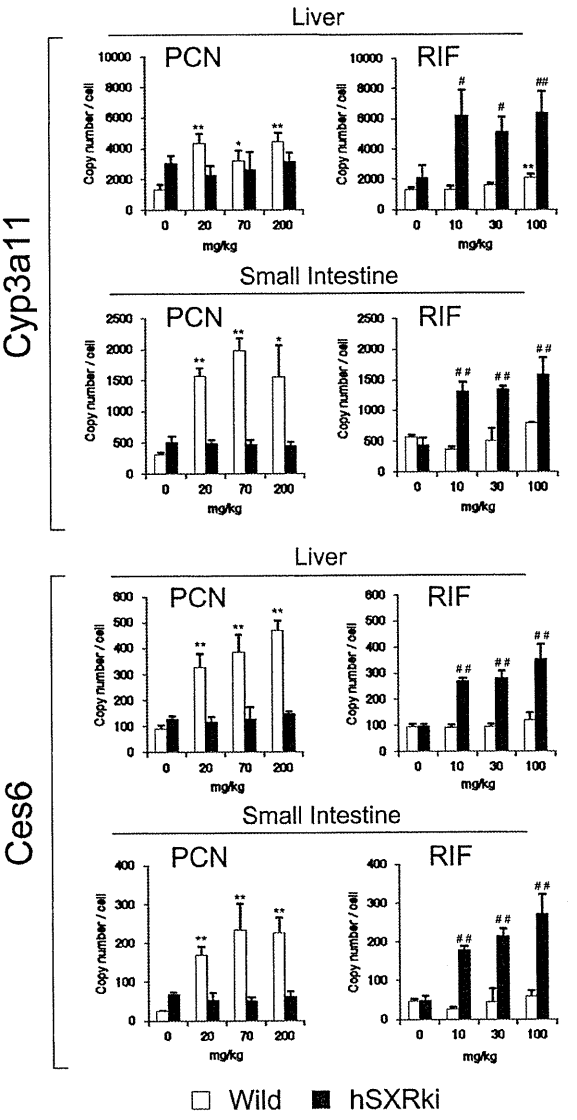

Fig. 3. Humanized response of hSXRki mice to RIF and PCN; Percellome quantitative RT-PCR. WT mice and hSXRki mice (n = 3 each) were singly dosed orally with vehicle (corn oil+0.1% DMSO), 20, 70, or 200 mg/kg PCN, or 10, 30, or 100 mg/kg of RIF (approximately equivalent in molar dose each other). Percellome quantitative RT-PCR data of Cyp3a11 and Ces6, both known as SXR target genes, in liver and small intestinal mucosa showed humanized responses in hSXRki. Bars = S.D., *; $p < 0.05$, **; $p < 0.01$ compared with vehicle group of WT, #; $p < 0.05$, ##; $p < 0.01$ compared with vehicle group of hSXRki. Analyzed by one-way ANOVA followed by Dunnett's post hoc comparison. Level of significance was set at $p < 0.05$.

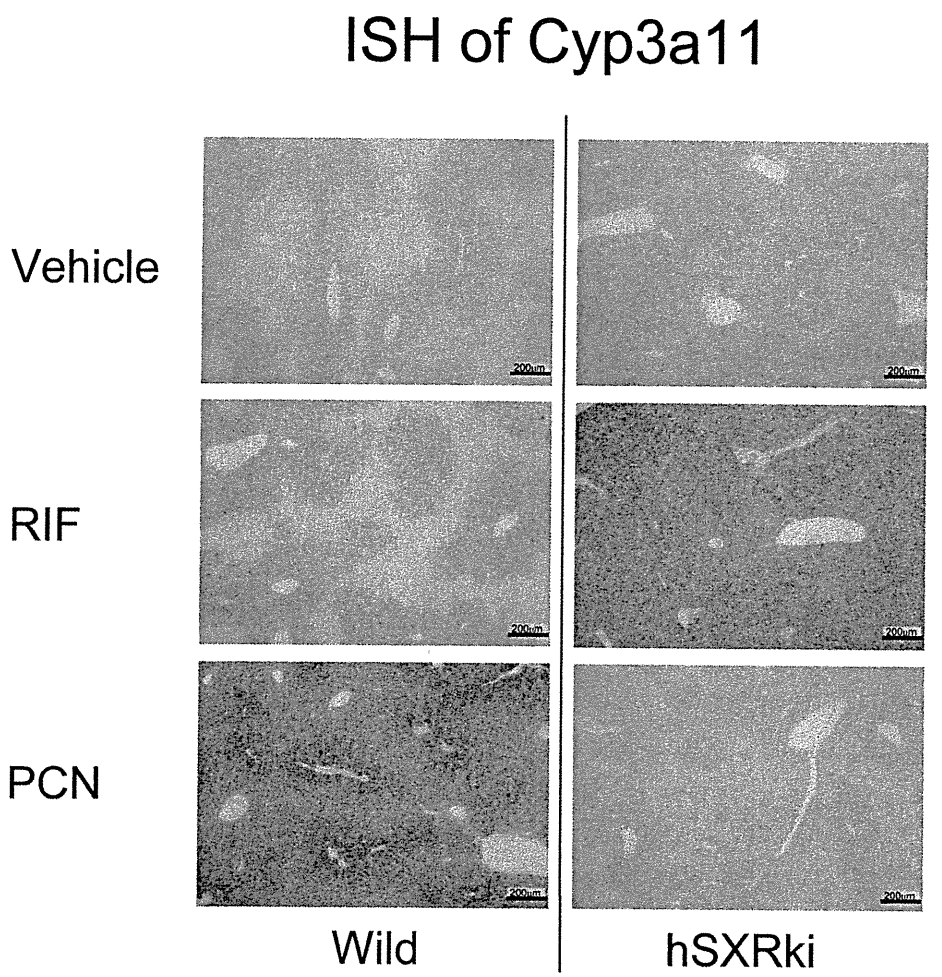

Fig. 4. Humanized response of hSXRki mice to RIF and PCN; *In situ* hybridization for Cyp3a11 mRNA in liver. A DIG-labeled cRNA probe for Cyp3a11 was hybridized and developed for purplish blue chromogenic reaction. Histologically, Cyp3a11 induction was localized around the central veins in both mice with species-specific ligands, respectively.

human-specific ligand RIF to the mice. Induction of the well-known SXR-regulated genes, Cyp3a11 and Ces6 was monitored by Percellome quantitative RT-PCR. As shown in Fig. 3, in the liver and small intestinal mucosa, RIF, but not PCN, induced Cyp3a11 and Ces6 in hSXRki mice (closed column), whereas PCN exclusively induced these genes in WT mice (open column). ISH of Cyp3a11 of the liver also showed humanized responses in hSXRki mice (Fig. 4).

DISCUSSION

We generated a new humanized mouse model in which the ligand binding domain (LBD) of human SXR was homologously knocked-into the murine SXR gene so that systemic response induced by human-selective SXR ligands can be monitored in mice. Firstly, we showed that mRNA from this chimeric gene was expressed at appropriate levels in the same tissues as the endogenous mouse SXR gene in WT mice. Then the humanized response of the mouse was confirmed by monitoring its response to the human-selective activator RIF, and the lack of response to the rodent-selective activator PCN.